Title: A new flatland buddy as toxic gas scavenger: a first principles study

Authors: Khushboo Patel, Basant Roondhe, Shweta D. Dabhi, Prafulla K. Jha

PII: S0304-3894(18)30150-X
DOI: https://doi.org/10.1016/j.jhazmat.2018.03.006
Reference: HAZMAT 19226

To appear in: *Journal of Hazardous Materials*

Received date: 28-10-2017
Revised date: 3-3-2018
Accepted date: 6-3-2018

Please cite this article as: Patel K, Roondhe B, Dabhi SD, Jha PK, A new flatland buddy as toxic gas scavenger: a first principles study, *Journal of Hazardous Materials* (2010), https://doi.org/10.1016/j.jhazmat.2018.03.006

A new flatland buddy as toxic gas scavenger: a first principles study

Khushboo Patel[1], Basant Roondhe[1], Shweta D Dabhi[2], Prafulla K Jha[1,#]

[1]Department of Physics, Faculty of Science, The M. S. University of Baroda, Vadodara-390 001

[2]Department of Physics, Maharaja Krishnakumarsinhji Bhavnagar University, Bhavnagar-364001

[#]Email: prafullaj@yahoo.com, pk.jha-phy@msubaroda.ac.in

Graphical Abstract

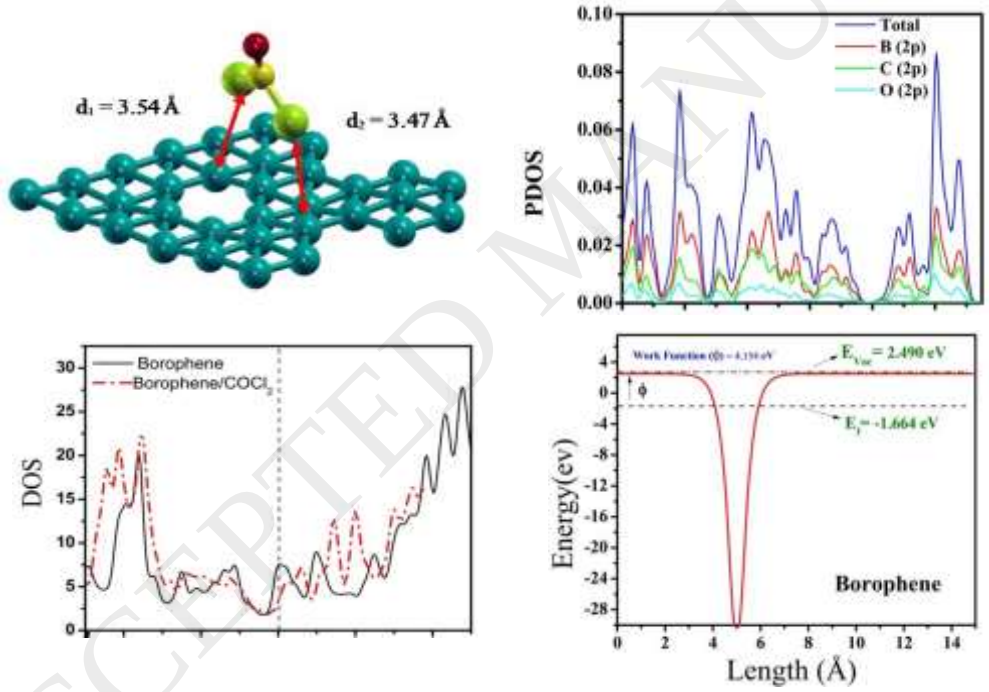

Highlights:

- Sensing behaviour of highly anisotropic borophene is investigated.
- Borophene interaction with toxic gases: phosgene and carbon monoxide.
- Structural and electronic properties of pristine and gas adsorbed borophene.
- Change in the work function of borophene over adsorption.

Abstract

Recently predicted and grown new single element two dimensional (2D) material borophene gathered tremendous research interest due to its structural, electronic and other properties. Using first principles based dispersion corrected density functional calculations, we have studied interaction of two toxic gases phosgene ($COCl_2$) and carbon monoxide (CO) with borophene to understand the role of borophene as biosensor and carriers in drug delivery. The sensing behaviour of borophene towards $COCl_2$ and CO has been studied by calculating the binding energy and electronic density of states (DOS). The change in the band structure, DOS, charge density and work function (WF) upon adsorption of gas molecules further confirms the sensing properties of borophene towards these molecules. The binding energy for $COCl_2$ and CO molecules on borophene is -0.306 eV and -0.15 eV respectively which indicates that the $COCl_2$ is adsorbed more favourably than CO over borophene. The WF is enhanced by 0.193 eV and 0.051 eV after the adsorption of $COCl_2$ and CO over borophene. Short recovery time of 148 ns and 37 ns for $COCl_2$ and CO has been predicted. The findings show that the borophene can be used as nanosensor to detect $COCl_2$ and CO.

Keywords: Borophene, Toxic gas, Work Function, $COCl_2$, CO, Sensor, Density Functional Theory.

1. Introduction:

From the past decade the development in the nanotechnology gets a thrust and the reason behind this thrust is the discovery of graphene. Since the successful isolation of graphene, two-dimensional (2D) materials have become a sizzling and active area of research in the nanomaterials and nanotechnology due to their potential for integration into next-generation electronic and energy conversion devices [1-4]. The most widely studied 2D material among all is Graphene with zero band gap and linear electronic dispersion at Dirac points [5]. The 2D carbon based material

graphene has attracted researchers due to its enormous properties like thermal conductivity [6], optoelectronic [7-8], charge carrier mobility [9-10], vibrational [11], thermal stability [12] etc., exceptionally different from its bulk counterpart. In particular, graphene has been considered as a candidate material for future electronics applications because of its extremely high carrier mobility and excellent electrode-channel contact [9-10]. However, the gapless intrinsic dispersion of graphene leads to an unacceptably high off-state current and a very low on/off ratio in graphene transistors. Although extensive efforts have been made to open a bandgap in different graphene nanostructures [13], the engineered bandgap critically depends on the atomic configurations of these structures. After rigorous research in the nanotechnology, several 2D materials like h-BN [14], transition metal dichalcogenides [15], silicene [16], germanene [17], arsenene [18], phosphorene [19], antimonene [20] etc. have been developed. The main reason which makes researchers to explore other similar 2D materials out of 3D materials is attention seeking properties of graphene.

More than a decade ago, borophene a structural cousin of graphene, has been predicted using density functional theory [21] and has recently been successfully synthesized using molecular beam epitaxy [22-23] and succeeds graphene. The synthesised borophene has a buckling structure [22]. The properties of borophene are very much similar to that of graphene such as light weight and exceptional strength but two of its properties make it superior over graphene such as its hollow hexagonal triangular lattice network which helps in tuning its mechanical properties by wearing the hollow hexagon concentration and its multicentre bonding. The properties of borophene are completely different from bulk boron as boron shows semiconducting behaviour while borophene is metallic at standard condition [24]. The strength and the properties of borophene can be tailored in very different ways, just by introducing more hollow hexagons (HHs) into the network. The low mass density, high strength, and high level of flexibility makes borophene a promising material for reinforcing elements for designing composites and for flexible nanodevices, such as flexible electrodes and contacts for nanoelectronics. The electronic, mechanical, magnetic and optical

properties of borophene have attracted tremendous interest [25-27]. Many sensors based on metal oxide semiconducting materials are available in the market for use in gas sensing applications due to their advantages such as low cost, low power consumption, easy to fabricate and high sensitivity towards many gases [28-30]. However, these materials have some limitation as they operate on elevated temperature up to 500° C [31], very long recovery time and limitation in the accuracy [32]. These limitations motivate scientists to find more efficient materials for the gas sensing applications due to high demand mainly arising from the rapid change in the environment. To fulfil these demands, the 2D materials have emerged as a possible solution as they possess high sensitivity towards many gases, low cost, low power consumption and the superior properties than conventional sensor material. The high surface to volume ratio feature of 2D materials provides large active surface for reaction with gas molecules, which helps to increase the sensor performance down to parts-per-billion (ppb) levels and make it frontier material for gas sensing applications [33].

The toxic and hazardous phosgene and carbon monoxide gases have been in regular use for manufacturing purposes in the industries. The highly hazardous carbon monoxide (CO) is generated due to the improper combustion. The detection of this gas is difficult because it is colourless, tasteless as well as odour less. The major source of its generation in the environment is from industrial activities, vehicles exhaust and the burning of fossil fuels. For human it is hazardous due to its attraction towards haemoglobin present in our blood. It enters in our body through breathing and reaches to our blood, resulting in the adsorption of all oxygen present in it which causes the malfunctioning of heart and brain because the oxygen required by them gets adsorbed by the CO gas [34]. The main symptom which can be seen when CO gets accumulated in our body is fatigue, headache etc. The high amount of CO in our body leads to damage our brain, unconsciousness and even death [35].

Phosgene ($COCl_2$) another toxic gas is used in the industries like polyurethane industries to

make isocyanate, pesticides, dye etc. [36]. Phosgene is quite dangerous due to its soothing odour which may not be noticed (as it is like fresh cut grass) and slow symptom. The detection of phosgene is done at 0.4ppm which is higher than the exposer limit of human. The reason behind the toxicity of phosgene to human is its harsh action towards the proteins which are present in the pulmonary alveoli. The interaction of the gas with the body causes damage to the blood-air barrier which causes suffocation [37].

The present work focuses on the exploration of a new 2D material borophene as a sensor for $COCl_2$ (Phosgene) and CO gases using state of the art first principles calculations based on density functional theory. The present first principles calculations based studies have been carried out to explore the most stable configuration for the adsorption of $COCl_2$ and CO over the borophene sheet and find the changes in its electronic and structural properties due to the interaction of adsorbed molecules. Of particular interest is to understand the interaction between two toxic gases and borophene sheet and find the possibility of using borophene to sense and detect toxic gases phosgene and carbon monoxide.

2. Computational Details:

The present study is done using first principles calculation under the frame work of density functional theory by employing the plane wave pseudopotential approach within the Generalized Gradient Approximation (GGA) [38] for exchange correlation functional as a part of the Quantum espresso code [39]. The kinetic energy and charge density cut off are 110 Ry and 1100 Ry respectively for single particle function in a plane wave basis set which helps in full convergence of all properties. The ultra-soft pseudopotentials are used for Cl, C, O and B. The Monkhorst and Pack [40] special grid point of 10x10x1 is used for Brillouin zone (BZ) integration. The optimized configuration of the pristine borophene has average B-B bond length of 1.69 Å. In the present study phosgene and carbon monoxide molecules which are toxic gases have been considered to

determine the sensing properties of borophene. A complete analysis has been done for full structure optimization, adsorption energy, electronic structure and density of states (DOS). Grimme's dispersion correction [41] is employed to consider the long range interactive force between the molecules and the nanosurface. The adsorption energy E_{ad} has been calculated according to the following equation

$$E_{ad} = E_{borophene+toxin} - (E_{borophene} + E_{toxin}) \quad (1)$$

Where $E_{borophene+toxin}$ is the total energy of borophene adsorbed by phosgene/carbon monoxide, $E_{borophene}$ is the total energy of the borophene sheet, E_{toxin} is the total energy of phosgene/carbon monoxide gas molecule obtained from optimization. According to the definition, $E_{ad} < 0$ indicates exothermic adsorptions.

3. Results and discussion

Before starting actual calculation of $COCl_2$ and CO molecules adsorbed borophene, we individually optimized borophene, $COCl_2$ and CO. Fig. 1(a) shows the optimized structure of borophene. The buckling is clearly observed in the **b** direction while there are no corrugations or any buckling along **a** direction. It can be seen from the Fig.1 (a) that the borophene has highly anisotropic crystal structure in contrast to other 2D honeycomb materials. It is important to know if the system over which dopant or molecule is to be adsorbed possesses dynamic stability or local minima. To understand the dynamical stability of any material phonon dispersion calculation plays an important role. Many properties like mechanical, acoustic, spectroscopic, thermodynamic and dynamical properties can be easily understand with the help of phonon dispersion curves (PDC). We have calculated the PDC for the borophene along with the phonon density of states (PHDOS) presented in Fig 1(b). There is a relation between the number of atom and the phonon branches in the dispersion curve, if there are N atoms in the unit cell, then we get 3N branches to the dispersion relation having 3 acoustical modes and 3N–3 optical modes [42]. Borophene consists of 8 atoms in the unit cell due to which there 24 phonon branches in the PDC including 3 acoustic and rest of 21 optical branches. The

characteristic acoustic phonon mods including out of plane ZA mode are obtain similar to graphene [43]. From the PDC it is clear that there is no imaginary phonon mods in the high symmetry direction of the BZ which confirms the dynamical stability of borophene. The highest frequency at **Γ** point is 1114 cm^{-1} arising due to the strong B-B bonding. The optical and acoustic branches of the dispersion have no gap due to homogeneous atom. The stability is further confirmed by calculating the PHDOS which is at the right panel of the Fig.1. The finite value of PHDOS at zero energy further confirms the absence of any imaginary phonon mods in entire BZ as its computation needs phonon frequencies in the entire Brillouin zone [44-45]. We have not calculated the phonon dispersion curves for adsorbed borophene systems which is not a serious drawback as having the system (borophene) over which molecule(s) which local minima is sufficient.

The optimized structures of $COCl_2$ and CO adsorbed borophene have been presented in Figs.2 (a) and (b) respectively. These figures clearly depict that the $COCl_2$ and CO prefers to be adsorbed on the surface and binds non-covalently above the hollow hexagon (HH) of the sheet as these molecules try to approach the vicinity of bare borophene. Furthermore, in the case of $COCl_2$ molecule Cl atoms prefer to be adsorbed on borophene (Fig.2 (a)), while both carbon and oxygen atoms of CO molecule prefer parallel orientation over borophene (Fig.2 (b)).

The electronic band structure of any material helps in understanding their electronic properties including moments of electron. Out of many, one of the main advantages of the band dispersion is to depict the mass of the electron whether it is finite or massless. The massless electron is only observed in the special case of Dirac bands [46] which results very high mobility of electron. Therefore, we have calculated the electronic band structure of pristine and gas molecules adsorbed borophene and shown in Fig.3 (a-c). The electronic properties are calculated along **k**-path **Γ−M−K−Γ** and the Dirac band is observed at **K** wave vector. The band structure depicts that the bands have large dispersions, which indicates small effective mass for electrons. It is observed that

in both cases $COCl_2$/CO adsorption on borophene causes a change in band structure. There are some bands which are crossing the Fermi level in Fig.3 (a) indicating metallicity of borophene. However, due to the adsorbed gases some impurity states within the band structure of the pristine borophene appear which is mainly due to the p electron of the O atom of the gas molecules as can be seen from the partial DOS presented in Fig.3 (b). Furthermore, there appear some flat bands in the conduction band region due to adsorption of the gas molecules. This can be attributed to the quenching of the kinetic energy of the electrons [47]. Further, the response of any sensor depends on the tuning of energy gap (E_g) which alters the electrical conductivity majorly responsible for any gas detection [48-51]

Fig.4 presents the density of states (DOS) together with the partial density of states (PDOS) for pristine as well as gas molecule adsorbed borophene for critical analysis of adsorption concentration. The side figures in Fig. 4 (a) show the enlarged DOS near Fermi level. These figures depict that the s-orbitals have little participation near the Fermi level of borophene while the p orbitals have the main contribution for the metallicity of borophene [52]. The metallic conductivities are maintained after adsorption. The DOS also shows an upward energy shift in the Fermi level of the borophene after gas molecule adsorption. Some extra peaks are observed for gas molecules adsorbed borophene in the energy region of 0.5−2.0 eV especially for carbon monoxide. The presence of these peaks suggests strong hybridization of borophene p and CO σ orbitals results from large electronic states near Fermi level. The dominant participation of p states as compared to s states can be seen in the Fig.4 (b).

To find the relative stability of the molecules over borophene, we have calculated the adsorption/binding energy of the gas molecules over borophene sheet. The binding energy (E_{ad}) of the adsorbed molecules $COCl_2$ and CO have been calculated using the total energies of bare and molecule adsorbed borophene sheet. The calculated results have been shown in Table I. It is clear from Table I that the phosgene gas molecule adsorption is energetically more favorable than the carbon monoxide. The calculated binding energy for phosgene is -0.306 eV while same for the CO

is -0.152 eV indicating that the adsorptions are ranging between weak chemisorption and strong physisorption. The calculated binding energy for $COCl_2$ adsorption on borophene is comparatively more than the $COCl_2$ adsorption over BNNT reported by J. Beheshtian et al. [53]. Their finding shows a weak binding of E_{ad} = -4.21 kcal/mol (0.18eV) for phosgene over BNNT which is almost half of the borophene case. However, adsorption energy (E_{ad} = -0.76 eV) is superior in the case of BNNT when doped with Sc [53]. The adsorption energy (E_{ad} = -1.058 eV) in the case of phosgene adsorbed over BNNR varies up to -6.0 eV by changing the adsorption site. The strong adsorption is due to the covalent interaction of phosgene with BNNR as at the open edge atoms as well as close edge atoms make covalent bonds with phosgene [54]. The CO adsorption over borophene is also comparatively higher than that of CO adoption over h-BN [55]. The adsorption on borophene is more due to its unique structure having an extra atom in the middle of the hexagonal geometry make several electronic states to cross the Fermi level and resulting into the metallic behaviour. The recent study of Liu et al. [56] on the effect of environmental gases like CO_2, NH_3, NO and NO_2 suggest that β12 borophene can interact with these gas and can be utilized as a sensor to sense these gases. In order to check the novelty of the present borophene sensor we have calculated the recovery time. The recovery time is one of the most important parameters which decide the superiority of any sensor with respect to the other sensor, which also plays an important role in its technology. The recovery time is generally measured by heating the sensor to higher temperature by experimentalist [57]. However, to estimate theoretically the recovery time of sensor following equation from transition theory is used.

$$\tau = \upsilon^{-1} e^{-E_{ads}/KT} \qquad (2)$$

Where υ is the attempt frequency, K is the Boltzmann constant (~8.318 $*10^{-3}$ kJ/mol K) and T is the temperature. From the previously reported work we have taken the attempt frequency of 10^{12} s^{-1} and temperature 298K, which has been employed to measure the recovery time for CNT from NO_2 molecule by Peng et al. [58]. We obtain relatively shorter recovery time of 37 ns and 148 ns for CO and $COCl_2$ respectively compare to other available sensors [59-60].

Major advantage of the charge density calculation is that it depicts the nature of the bonding. The charge density behavior of the chemical bonding and charge transfer has been calculated in (101) and (110) plane for $COCl_2$/borophene and CO/borophene systems respectively. The charge density plots are shown in Fig. 5. The electronegativity value for $COCl_2$ gas is around 0.974 and for borophene sheet is 0.063. The plot shows that there is no bonding between the gas molecule and the borophene sheet. The maximum charge is accumulated near the oxygen atom of $COCl_2$ (+0.974). The accumulation of charge near oxygen atom suggests that oxygen contribute significantly in the charge density than Chlorine and Carbon. The charge transfer occurs from borophene to molecules as these molecules are of oxidizing nature. When the $COCl_2$ is adsorbed over borophene there is a charge transfer of 0.055e and in the case of the CO adsorption charge transfer of 0.048e is observed. Similar conclusion is drawn from DOS.

For the further proof of the sensing capability of borophene towards $COCl_2$ and CO toxic gases, we have studied the change in work function (WF) of the system. The WF of a metal/ semiconductor is the least amount of energy required to free an electron from its Fermi level to a point which is outside the material (vacuum). As the WF is surface dependent, it can also define the sensing property of the surface at which the adsorption takes place because it strongly affects the conduction of the surface of material. The change in WF of borophene after adsorption alters its conducting properties. Fig. 6 shows a schematic WF diagram of pristine borophene and CO and $COCl_2$ adsorbed borophene, in which valence bands are filled with electrons up to the Fermi energy (E_f). WF values are calculated using following equation [61]

$$\phi = E_{inf} - E_F \qquad (3)$$

where E_{inf} is the electrostatic potential at infinity (outside the material) or vacuum and E_F is the Fermi level energy. The result of the WF calculation is shown in Table 1. The results reveal that the calculated work function of pristine borophene which is 4.154 eV undergoes a significant change after adsorption of both gases. The value changes to 4.205 eV and 4.347 eV on the adsorption of CO and $COCl_2$ respectively. The change in WF is ($\Delta\phi$) which is calculated by subtracting the WF of

pristine borophene and the WF of adsorbed borophene with gases CO and $COCl_2$ is 0.051 eV and 0.193 eV respectively. This $\Delta\phi$ clearly depicts the influence of these adsorbents on pristine borophene. Interestingly in both cases the WF of the pristine borophene is increased which may arise because of the removal of charge from borophene sheet by two adsorbents CO and $COCl_2$ as these adsorbents are oxidizing gases. The WF we obtained for pristine borophene is 4.154 eV which is in good agreement with previous theoretical work (4.09 eV) [62] and experimental data (4.02 eV) [63]. From the results we get to know that the $COCl_2$ shows more alteration in the WF of pristine borophene than CO.

Thus, a reliable conclusion which is drawn by our calculations is that it provides a solid support that both the carbon monoxide and phosgene gas molecules modifies the electronic properties of borophene and the newly develop 2D material borophene will be the next generation gas scavenger especially for toxic gas like phosgene and can be utilize as improved sensor for the future.

4. Conclusions:

In summary the present study reports a Van der Waals corrected density functional theory based first principles calculation to understand the interaction of two toxic gas molecules $COCl_2$ and CO with 2D material borophene and find the possibility of using it as sensor to sense and detect these toxic gases. Upon adsorption of $COCl_2$ and CO on the borophene sheet, they prefer to be adsorbed on the surface and binds non-covalently above the hollow hexagon of the sheet. In addition Cl atom of $COCl_2$ molecule prefers borophene but both carbon and oxygen of CO prefer parallel orientation. The electronic band structures show the presence of large electronic states near the Fermi levels arising from strong hybridization of borophene p and CO sigma orbit which results into the sharp peaks in the region of 0.5 – 2.0 eV especially for CO. The obtained results on adsorption energy indicates that the both CO and $COCl_2$ gas molecules show physisorption over borophene but the interaction between $COCl_2$ and borophene is stronger as compared to CO. Short recovery time of 37 ns and 148 ns for CO and $COCl_2$ confirms the superiority of borophene for the use as a sensor.

Furthermore, the shift in the Fermi energy which plays a crucial role in the determination of work function is dominant cause leading to increase the work function. This suggests that the sensitivity and selectivity of borophene-based gas sensors could be the next new material for gas sensing application. The sensing of borophene towards $COCl_2$ and CO is better in borophene compared to BNNT as well as BNNR attributed to the metallicity and ionic character of borophene.

Acknowledgments

Financial assistance from the SERB, Govt. of India, through grant SR/S2/CMP-0005/2013 is acknowledged. Part of the computations is carried out using high performance computer cluster provided under DST-FIST program.

References

1. Novoselov, K. S.; Geim, A. K.; Morozov, S. V. Electric field effect in atomically thin carbon films. *Science* **2004**, 306, 666-669.
2. Novoselov, K. S.; Fal'ko, V. I.; Colombo, L.; Gellert, P. R.; Schwab, M. G.; Kim, K. A roadmap for graphene. *Nature* **2012** 490**,** 192-200.
3. Klinovaja, J.; Loss, D. Spintronics in MoS_2 monolayer quantum wires. *Phys. Rev. B* **2013**, 88, 075404-075410.
4. Xu, Y.; Gan, Z.; Zhang, S.-C. Enhanced thermoelectric performance and anomalous seebeck effect in topological insulators. *Phys. Rev. Lett.***2014**, 112, 226801-226805.
5. Novoselov, K. S.; Geim, A. K.; Morozov, S. V.; Jiang, D.; Katsnelson, M. I.; Grigorieva, I. V.; Dubonos, S. V.; Firsov, A. A. Two-dimensional gas of massless dirac fermions in graphene. *Nature* **2005**, 438, 197-200.
6. Pop, E; Varshney, V; Roy, A. K. Thermal properties of graphene: Fundamentals and applications. *MRS Bull.***2012**, 37, 1273-1281.
7. Wang, X; Zhi, L; Mullen, K. Transparent, conductive graphene electrodes for dye-sensitized solar cells. *Nano Letters* **2008**, 8, 323–327.
8. Chen, J.H.; Ishigami. M; Jang, C; Hines, D. R; Fuhrer, M. S.; Williams ED. Printed graphene circuits. *Adv Mater* **2007**, 19, 3623–3627.
9. Morozov, S. V.; Novoselov, K. S.; Katsnelson, M. I.; Schedin, F; Elias, D. C.; Jaszczak, J. A.; Geim. A. K. Giant intrinsic carrier mobilities in graphene and its bilayer. *Phys Rev Lett* **2008**, 100, 016602-016605.
10. Chen, J. H.; Jang, C.; Adam, S.; Fuhrer, M. S.; Williams, E. D.; Ishigami, M. Charged-impurity scattering in graphene. *Nat Phys* **2008**, 4, 377–381.
11. Wang, H.; Wang, Y.; Cao, X.; Feng, M.; Lan, G. Vibrational properties of graphene and graphene layers. *J. Raman Spectrosc*. **2009**, 40, 1791–1796.
12. Nan, H. Y.; Ni, Z. H.; Wang, J,; Zafar, Z,; Shi, Z. X.; Wang, Y. Y. The thermal

stability of graphene in air investigated by Raman spectroscopy. *J. Raman Spectrosc*. **2013**, 44, 1018–1021.

13. Molitor, F; Güttinger, J; Stampfer, C; Dröscher, S; Jacobsen, A; Ihn, T; Ensslin, K. Electronic properties of graphene nanostructure. *Phys.: Condens. Matter* **2011**, 23, 243201-243215.
14. Xu, Y. N.; Ching, W. Y. Calculation of ground-state and optical properties of boron nitrides in the hexagonal, cubic, and wurtzite structures. *Phys. Rev. B* **1991,** 44, 7787–7798.
15. Choi, W.; Choudhary, N.; Han, G. H.; Park, J; Akinwande, D.; Lee, Y. H. Recent development of two-dimensional transition metal dichalcogenides and their applications. *mater. Today* **2017**, 20, 116-130.
16. Takeda, K.; Shiraishi, K. Theoretical possibility of stage corrugation in Si and Ge analogs of graphite. *Phys. Rev. B* **1994**, 50, 14916-14922.
17. Cahangirov, S.; Topsakal, M.; Akturk, E.; Sahin, H.; Ciraci, S. Two and one-dimensional honeycomb structures of silicon and germanium. *Phys. Rev. Lett.* **2009**, 102, 236804-236808.
18. Zhang, S.; Zhong, Y.; Li, Y.; Chen, Z.; Zeng, H. Atomically thin arsenene and antimonene: Semimetal-semiconductor and indirect-direct band-gap transitions. *Angew. Chem., Int. Ed. Engl*. **2015**, 54, 3112-3115.
19. Liu, H.; Neal, A. T.; Zhu, Z.; Luo, Z.; Xu, X.; Toma´nek, D.; Ye, P. D. Phosphorene: an unexplored 2D semiconductor with a high hole mobility. *ACS Nano* **2014**, 8, 4033–4041.
20. Kamal, C.; Ezawa, M. Arsenene: Two-dimensional buckled and puckered honeycomb arsenic systems. *Phys. Rev. B* **2015**, 91, 085423-085432.
21. Tang, H.; Ismail-Beigi, S. Novel precursors for boron nanotubes: the competition of two-center and three-center bonding. *Phys. Rev. Lett.* **2007**, 99, 115501-115504.

22. Mannix, A. J.; Zhou, X. F.; Kiraly, B.; Wood, J. D.; Alducin, D.; Myers, B. D.; Liu, X.; Fisher, B. L.; Santiago, U.; Guest, J. R. Synthesis of borophenes: Anisotropic, two-dimensional boron polymorphs. *Science* **2015**, 350, 1513-1516.

23. Feng, B.; Zhang, J.; Zhong, Q.; Li, W.; Li, S.; Li, H.; Cheng, P.; Meng, S.; Chen, L.; Wu, K. Experimental realization of two-dimensional boron sheets. *Nat. Chem.* **2016**, 8, 563-568.

24. Feng, B.; Zhang, J.; Liu, R. Y.; Iimori, T.; Lian, C.; Li, H.; Chen, L.; Wu, K.; Meng, S.; Komori, F. Direct evidence of metallic bands in a monolayer boron sheet. *Phys. Rev. B* **2016**, 94, 041408-041412.

25. Peng, B.; Zhang, H.; Shao, H.; Xu, Y.; Zhanga, R.; Zhua, H. The electronic, optical, and thermodynamic properties of borophene from first-principles calculations. *J. Mater. Chem. C* **2016**, 4, 3592-3598.

26. Lherbier, A.; Botello-Mndez, A. R.; Charlier, J. C. Electronic and optical properties of pristine and oxidized borophene. *2D Materials* **2016**, 3, 045006-045014.

27. Zhou, Y. P.; Jiang, J-W. Molecular dynamics simulations for mechanical properties of borophene: parameterization of valence force field model and Stillinger-Weber potential. *Scientific Reports* **2017**, **7**, 45516-45527.

28. Siyama, T.; Kato, A. A new detector for gaseous components using semiconductor thin film. *Anal. Chem.* **1962**, 34, 1502–1503.

29. Tomchenko, A.A.; Harmer, G.P.; Marquis, B.T.; Allen, J.W. Semiconducting metal oxide sensor array for the selective detection of combustion gases. *Sens. Actuators B* **2003**, 93,126–134.

30. Arafat, M.; Dinan, B.; Akbar, S.A.; Haseeb, A. Gas sensors based on one dimensional nanostructured metal-oxides: *A review. Sensors* **2012**, 12, 7207–7258.

31. Barsan, N.; Weimar, U. Conduction model of metal oxide gas sensors. *J. Electroceramics* **2001**, 7, 143–167.

32. Capone, S.; Forleo, A.; Francioso, L.; Rella, R.; Siciliano, P.; Spadavecchia, J.; Presicce, D.; Taurino, A. Solid state gas sensors: State of the art and future activities. *J. Optoelectron. Adv. Mater.* **2003**, 5, 1335–1348.

33. Jimenez-Cadena, G.; Riu, J.; Rius, F. X. Gas sensors based on nanostructured *materials. Analyst* **2007**, 132, 1083–1099.

34. Tikuisis, P.; Kane, D. M.; McLellan, T. M.; Buick, F.; Fairburn, S. M. Rate of formation of carboxyhemoglobin in exercising humans exposed to carbon monoxide. *Journal of Applied Physiology* **1992**, 72, 1311–1319.

35. Ernst A.; Zibrak, J. D. Carbon monoxide posioning. *The New England Journal of Medicine* **1998**, 339, 1603–1608.

36. Shriner, R. L.; Horne, W. H.; Cox, R. F. B. p-Nitrophenyl Isocyanate. *Org. Synth. Coll.* **1943**, 2, 453-455.

37. Schneider, W.; Diller, W. "Phosgene", Ullmann's Encyclopedia of Industrial Chemistry, Weinheim: Wiley-VCH, **2005** doi:10.1002/14356007.a19_411.

38. Perdew, J. P.; Burke, K.; Ernzerhof, M. Generalized Gradient Approximation Made Simple. *Phys. Rev. Lett.* **1996**, 77, 3865-3868.

39. Giannozzi, P. et al. QUANTUM ESPRESSO: a modular and open-source software project for quantum simulations of materials. *J. Phys.: Condens. Matter* **2009**, 21, 395502-395520.

40. Monkhorst, H. J.; Pack, J. D. Special points for Brillonin-zone integration. *Phys .Rev. B* **1976**, 13, 5188-5192.

41. Grimme, S.; Antony, J.; Ehrlich, S.; Krieg, H. A consistent and accurate ab initio parametrization of density functional dispersion correction (DFT-D) for the 94 elements H-Pu. *The Journal of Chemical Physics* **2010**, 132, 154104-154122.

42. Kittel, C. Introduction to Solid State Physics, Ch. 4, 95–98 (Wiley, 2005).

43. Gupta, S. K.; Soni, H. R.; Jha, P. K. Electronic and phonon bandstructures of pristine

few layer and metal doped graphene using first principles calculations. *AIP Advances* **2013**, 3, 032117-032132.

44. Jha, P. K; Sanyal, S. P. Phonon spectrum and lattice specific heat of the $HgBa_2CuO_4$ high-temperature superconductor. *Physica C: Superconductivity* **1996**, 271, 6-10.
45. Jha, P. K. Phonon spectra and vibrational mode instability of MgCNi3. *Phys. Rev. B* **2005**, 72, 214502-214507.
46. Geim, A. K.; Novoselov, K. S. The rise of graphene. *Nat Mater.* **2007**, 6, 183-191.
47. Gulacsi, Z. Interaction created effective flat bands in conducting polymers. *Eur. Phys. Jour. B* **2014,** 87, 143-165.
48. Beheshtian, J.; Peyghan, A. A.; Bagheri, Z. Sensing behavior of Al-rich AlN nanotube toward hydrogen cyanide. *J Mol Model* **2013,** 19, 2197-2203.
49. Bagheri, Z.; Peyghan, A. A. DFT study of NO2 adsorption on the AlN nanocones *Comput. Theor. Chem.* **2013**, 1008, 20-26.
50. Peyghan, A. A.; Rastegar, S. F.; Hadipour N. L. DFT study of NH3 adsorption on pristine, Ni- and Si-doped graphynes. *Physics Letters A* **2014**, 378, 2184-2190.
51. Eslami, M.; Peyghan, A. A. DNA nucleobase interaction with graphene like BC3 nano-sheet based on density functional theory calculations. *Thin Solid Films* **2015**, 589, 52-56.
52. Zhang, X.; Hu, J.; Cheng, Y.; Yang, H. Y.; Yao, Y.; Yang, S. A. Borophene as an extremely high capacity electrode material for Li-ion and Na-ion batteries. *Nanoscale* **2016**, 8, 15340-15347.
53. Beheshtiana, J.; Peyghanb, A. A.; Bagheric, Z. Detection of phosgene by Sc-doped BN nanotubes: A DFT study. *Sensors and Actuators B: Chemical* **2012**, 171, 846–852.
54. Srivastava, P.; Sharma, V.; Jaiswal, N. K. Adsorption of COCl2 gas molecule on armchair boron nitride nanoribbons for nano sensor applications. *Microelectronic*

Engineering **2015**, 146, 62–67.

55. Pashangpour, M. IPCBEE vol.2 © (2011) IACSIT Press, Singapore.
56. Liu, T.; Chen, Y.; Zhang, M.; Yuan, L.; Zhang, C.; Wang, J.; Fan, J. A first-principles study of gas molecule adsorption on borophene. *AIP Advances* **2017**, 7, 125007-125015.
57. Rostami, Z.; Pashangpour, M.; Moeadi, R. DFT study on the chemical sensing properties of B24N24 nanocage toward formaldehyde. *J. Mol. Graph. Model.* **2017**, 72, 129–135.
58. Peng, S.; Cho, K.; Qi, P.; Dai, H. Ab initio study of CNT NO2 gas sensor. *Chem. Phys. Lett.* **2004**, 387, 271–276.
59. Aghaei, S. M.; Monshi, M.M.; Torres, I.; Zeidi, S.M.J.; Calizoa, I. DFT study of adsorption behavior of NO, CO, NO2, and NH3 molecules on graphene-like BC3: A search for highly sensitive molecular sensor. *Appl. Surf. Sci.* **2018**, 427, 326–333.
60. Vessally, E.; Moladoust, R.; Mousavi-Khoshdel, S. M.; Esrafili, M. D.; Hosseinian, A.; Edjlali, L. Chloropicrin sensor based on the pristine BN nanocones: DFT studies. *Struct. Chem.* **2017**, 28, 1-8.
61. Lang, N. D.; Kohn,W. Theory of Metal Surfaces: Work Function. *Phys. Rev. B* **1971**, 3, 1215-1223.
62. Bezugly, V.; Kunstmann, J.; Grundkötter-Stock, B.; Frauenheim, T.; Niehaus, T.; Cuniberti, G. Highly Conductive Boron Nanotubes: Transport Properties, Work Functions, and Structural Stabilities. *ACS Nano* **2011**, 5, 4997−5005.
63. Liu, F.; Shen, C.; Su, Z.; Ding, X.; Deng, S.; Chen, J.; Xu, N.; Gao, H. Metal-Like Single Crystalline Boron Nanotubes: Synthesis and In Situ Study on Electric Transport and Field Emission Properties. *J. Mater. Chem.* **2010**, 20, 2197−2205.

Figure Caption

Figure1: (a) Optimized structure of borophene (dashed line shows the unite cell) (side view and top view) and (b) phonon dispersion curve along with phonon density of states (PHDOS).

Figure2: (a) Optimized structure of borophene adsorbed $COCl_2$ gas molecule (side view and top view).

(b) Optimized structure of borophene adsorbed CO gas molecule (side view and top view).

Figure3: (a) Band structure of pristine borophene. Red colour shows the conduction band and the blue colour shows the valance band

(b) Band structure of $COCl_2$ adsorbed borophene. Red colour shows the conduction band and the blue colour shows the valance band.

(c) Band structure of CO adsorbed borophene. Red colour shows the conduction band and the blue colour shows the valance band.

Figure4: (a) Density of states (DOS) plot of pristine borophene and the functionalized borophene with $COCl_2$ and CO (inset shows shift in the density of states at Fermi). (b) Projected Density of states (PDOS) plot of pristine borophene and the functionalized borophene with $COCl_2$ and CO.

Figure5: Charge density plots (a) CO/Borophene and (b) $COCl_2$/Borophene.

Figure6: Work function plot of (a) pristine borophene, Work function plot of adsorbed borophene with (b) $COCl_2$ and (c) CO.

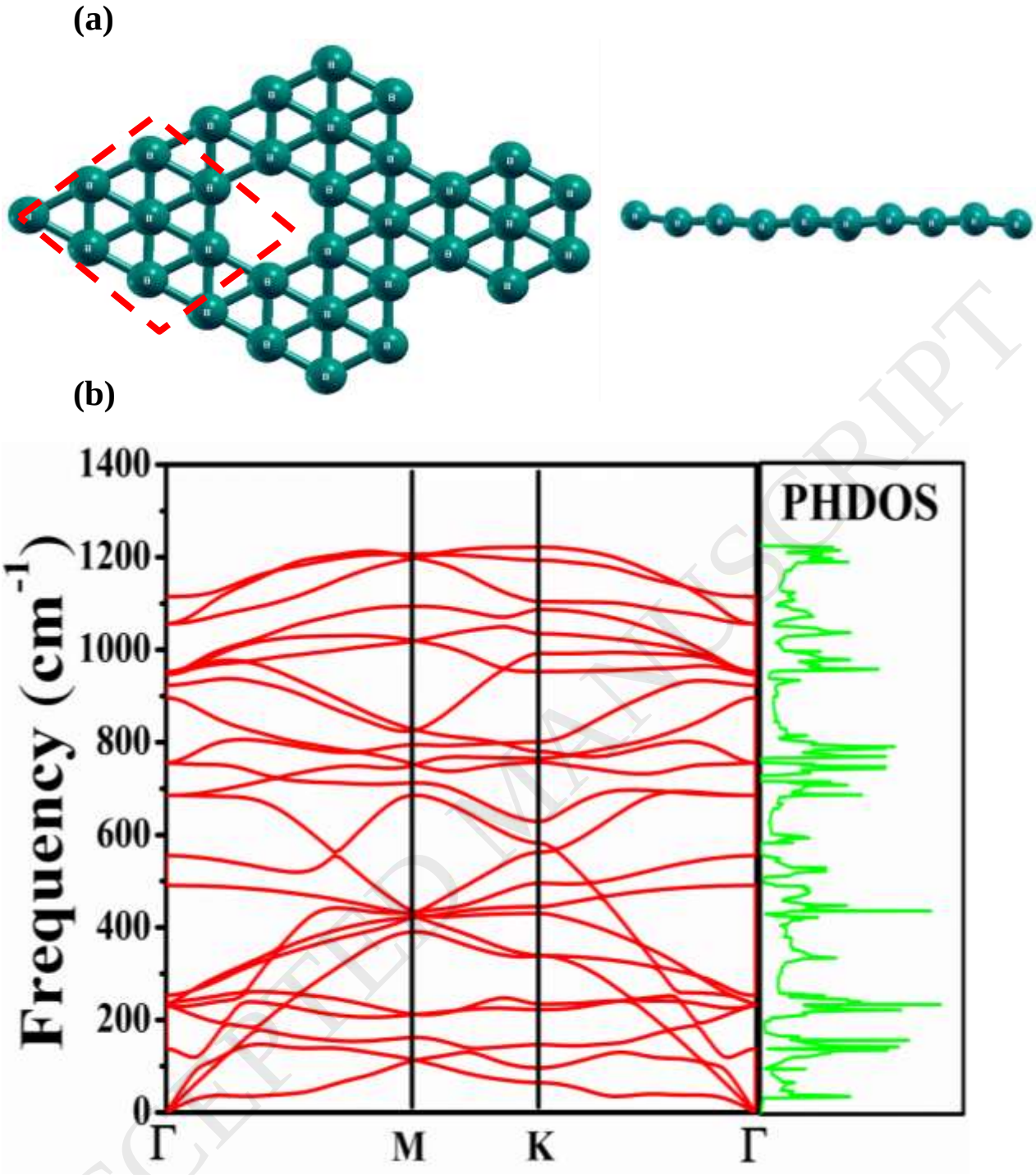

Fig.1

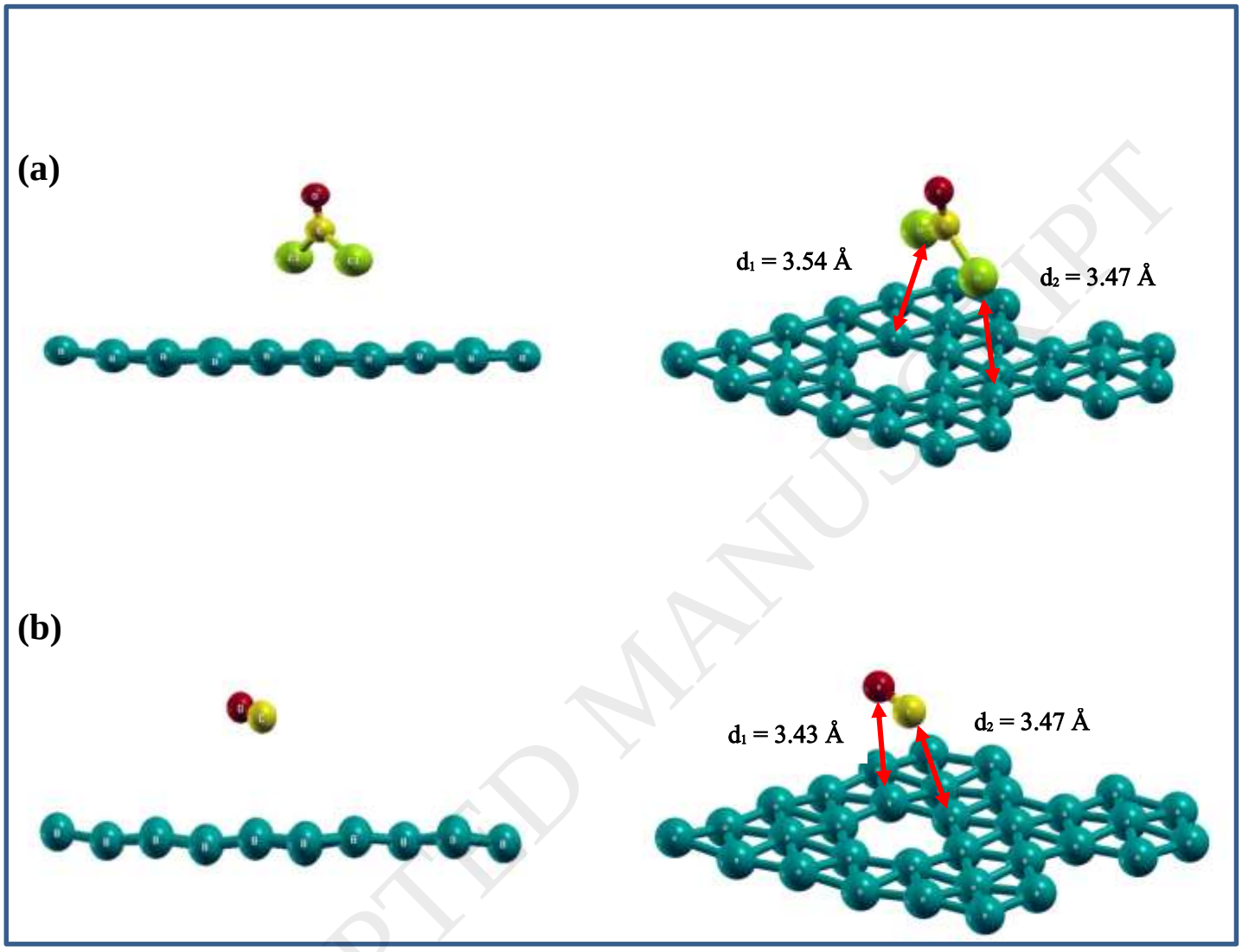

Fig.2

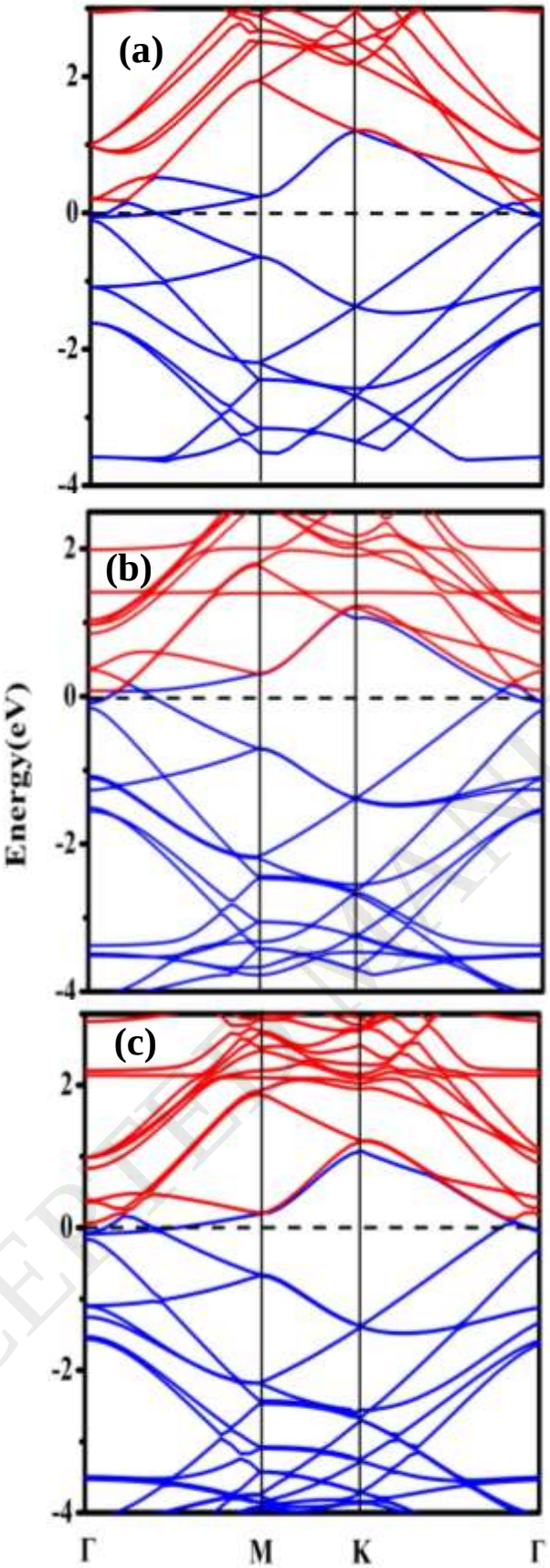

Fig.3

(a)

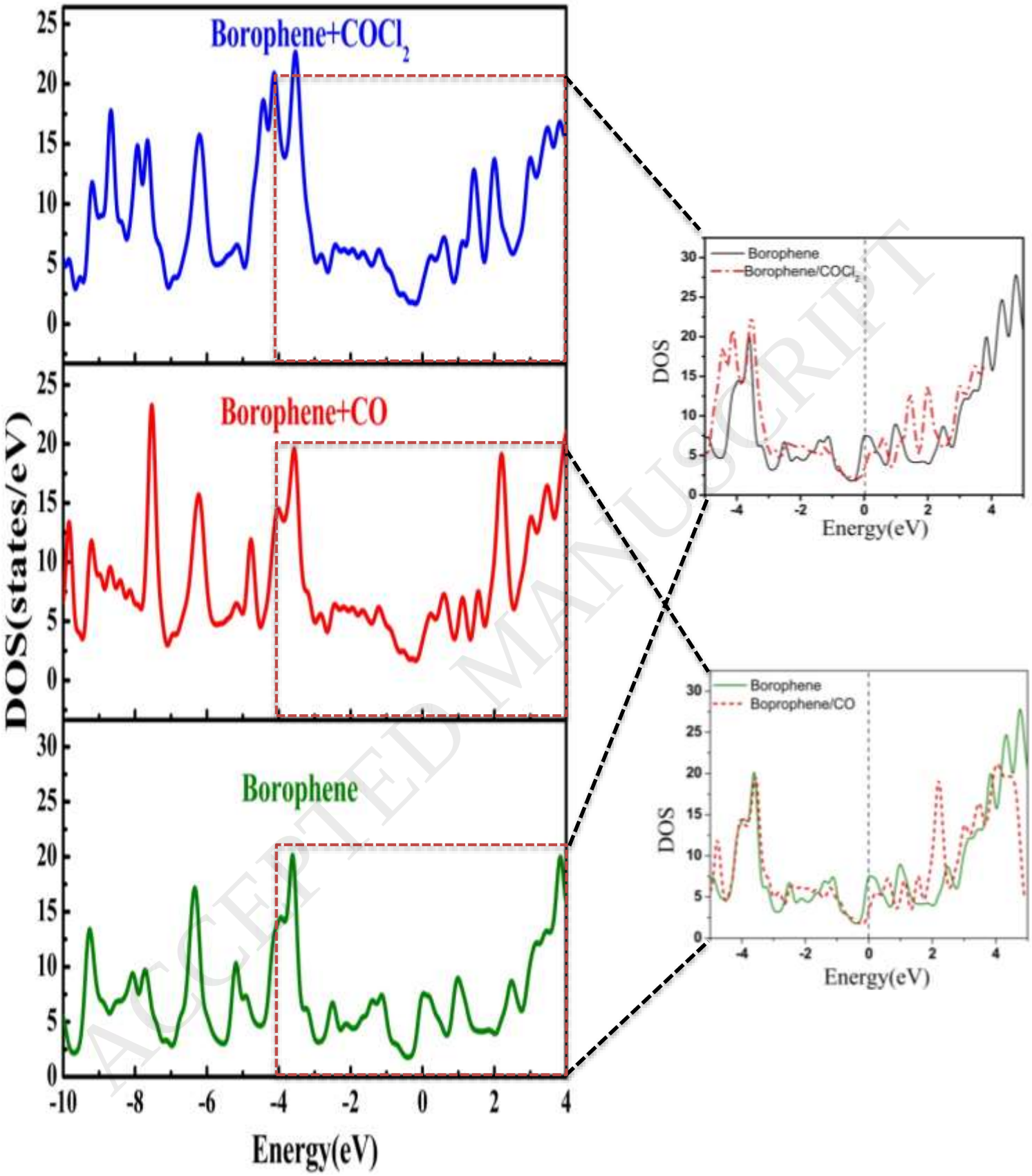

(b)

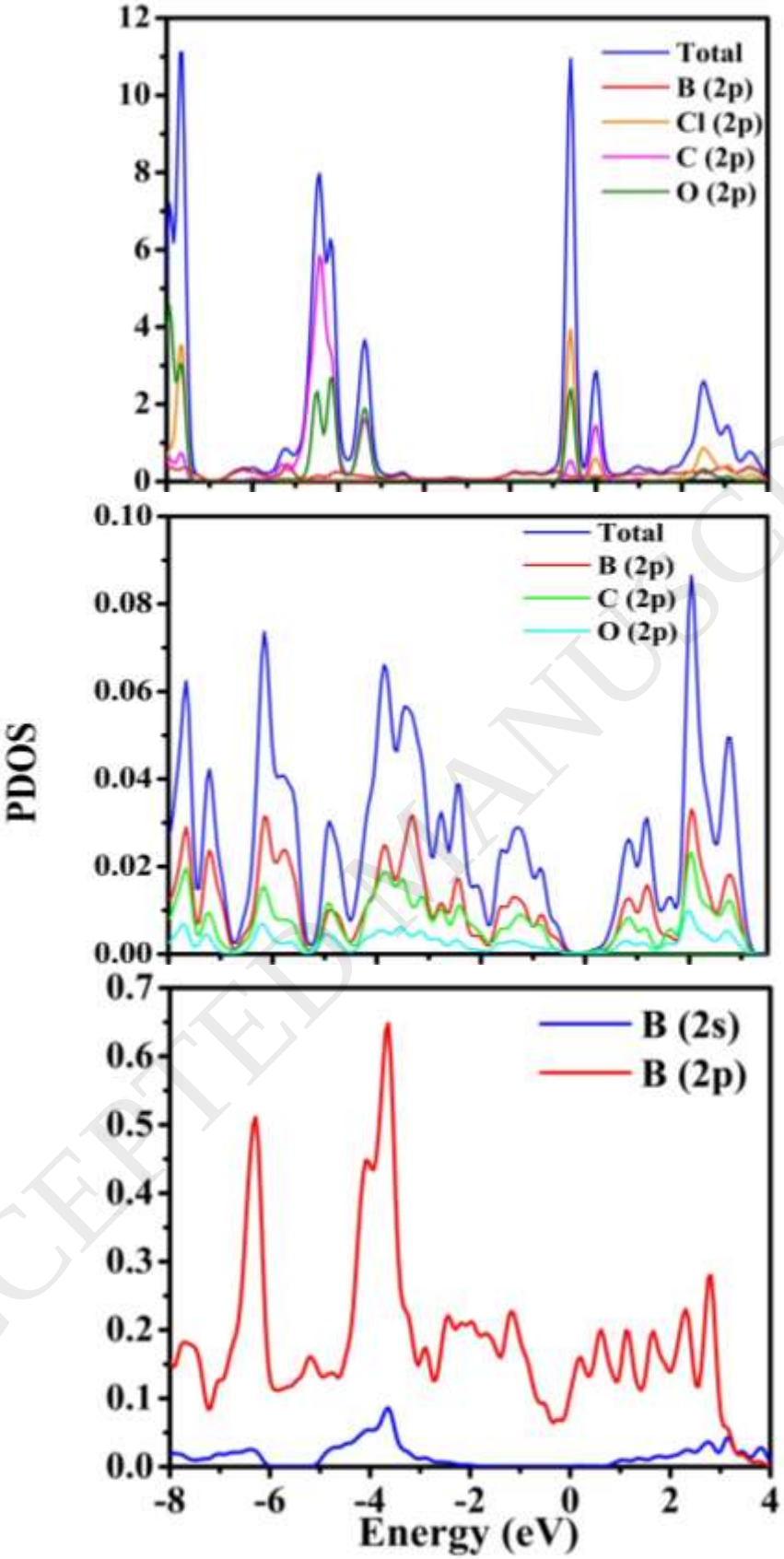

Fig.4

(a)

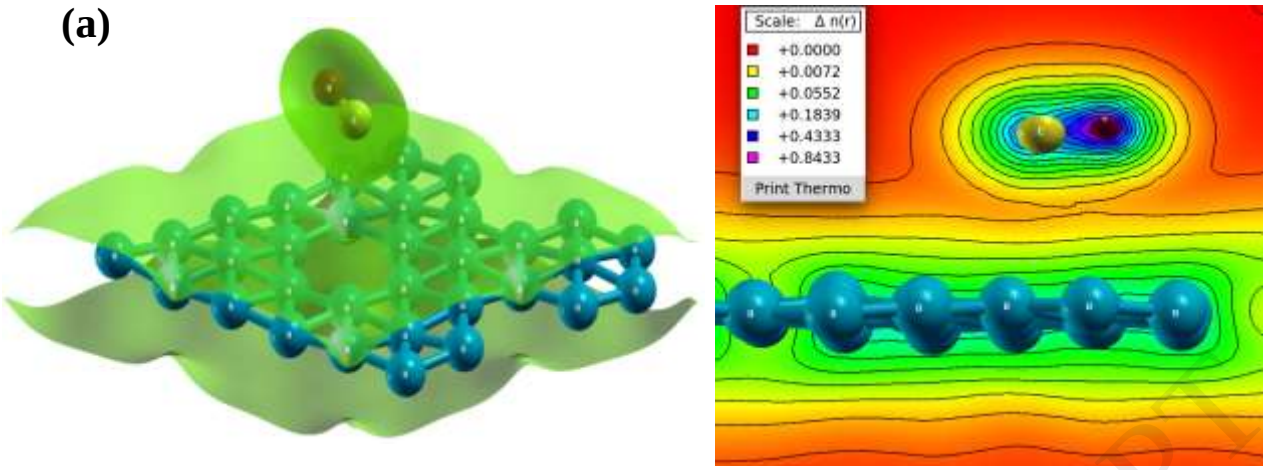

(b)

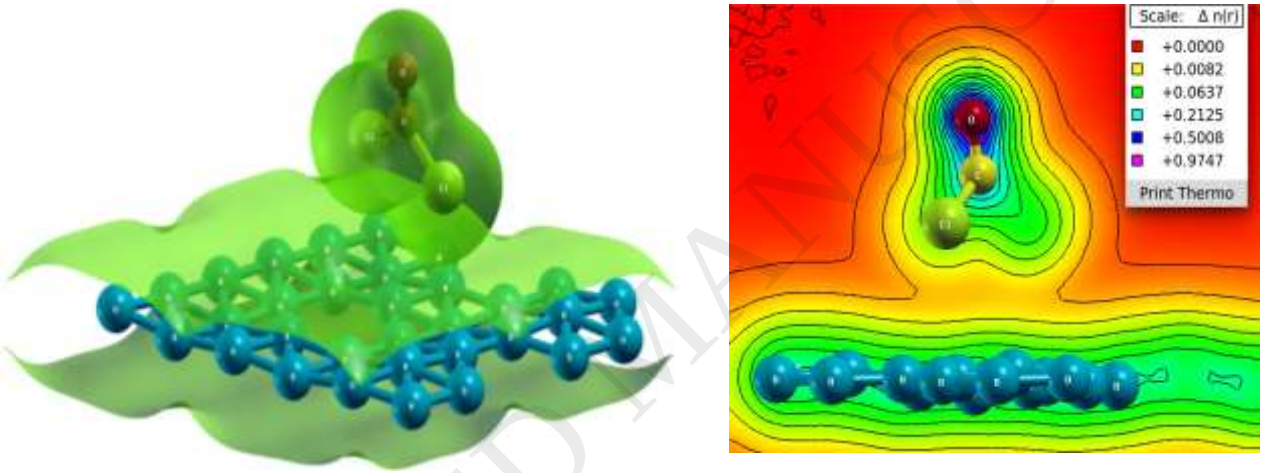

Fig.5

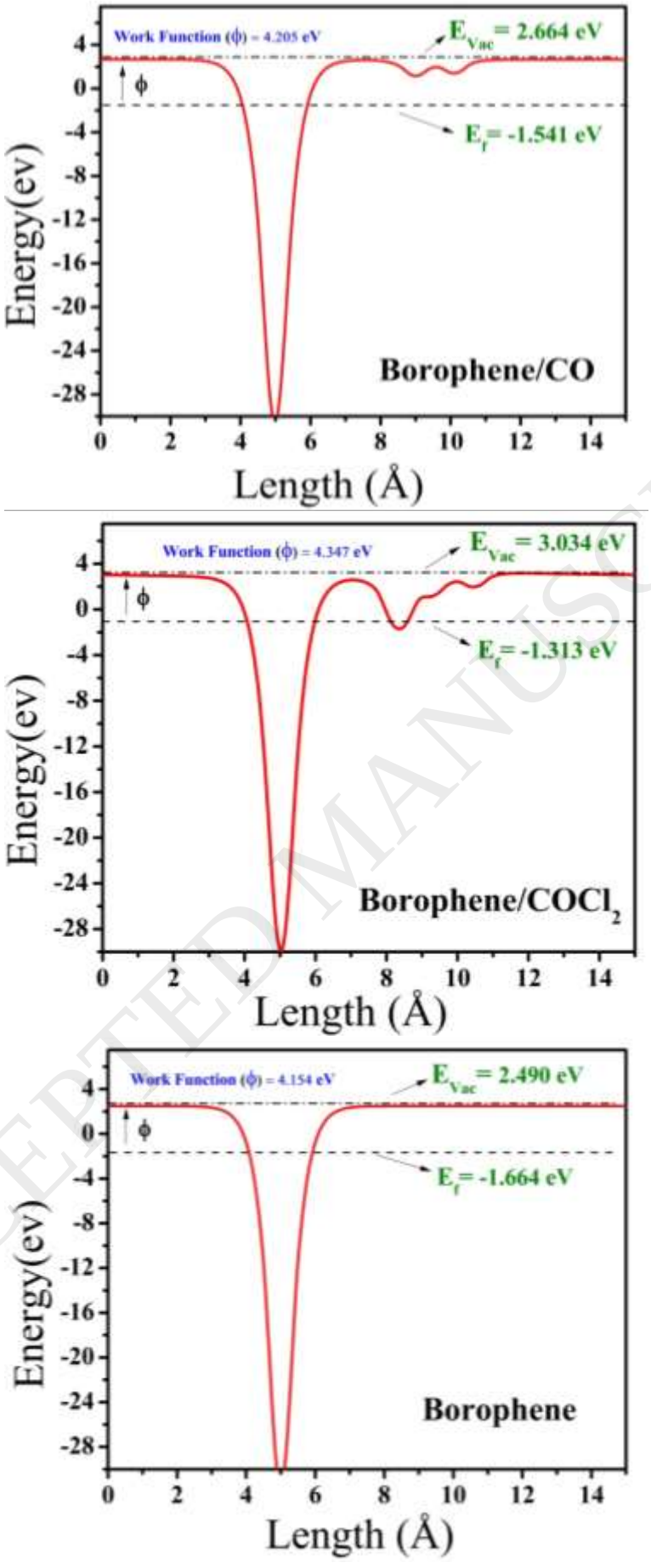

Fig.6

Table1. Calculated energetic data binding energies (E_{ad}), Fermi level energies (E_F) and Work function (E_{wf}).

System	E_F (eV)	E_{wf} (eV)	E_{ad} (eV)
Borophene	-1.664	4.154	-
Borophene +CO	-1.541	4.205	-0.152
Borophene +$COCl_2$	-1.313	4.347	-0.306